BRAID-TRUSION OF HOLLOW GLASS FIBRE / POLYETHYLENE TEREPHTHALATE THERMOPLASTIC COMPOSITES

Maissaloun El-Jakl[1*] and Louis Laberge Lebel[1]

[1] Advanced Composites and Fibres Structures Laboratory (ACFSlab), High Performance Polymer and Composite Systems (CREPEC), Polytechnique Montreal, 2500 ch Polytechnique, Montreal, Qc, Canada, H3T 1J4

* Corresponding author (Maissaloun.el-jakl@polymtl.ca)

Keywords: Braid, Pultrusion, thermoplastic composite, hollow structure, DREF

ABSTRACT

Braid-trusion is a manufacturing process for composite materials. It involves pulling braids through a pultrusion die to continuously manufacture structures with a constant cross-section and angle-oriented fibres. In the pultrusion process, these braids are subjected to tension and compression, which lead to braid deformation and alterations in the fibre orientation. Fibre orientation is a crucial factor in determining the mechanical properties of a composite. Defects such as wrinkling or fibre waviness can also occur during braid consolidation, resulting in a deterioration of the properties of the composite. The aim of this study is to limit fibre waviness using an internal consolidation approach. Glass fibre/polyethylene terephthalate DREF yarns were triaxially braided around mandrels of different diameters. Hollow braided structures were pultruded through a multi-die process using either external or internal consolidation. The pultrusion mandrel used for internal consolidation had an ascending cross-section with an initial circumference of 90% its finale one. The braiding machine parameters were adjusted to obtain a pitch of 80 mm for all braids. After pultrusion, internal and external surfaces were assessed for fibre waviness. It was seen that braid-truded hollow structures made using external consolidation show a high fibre waviness compared to tubes made using internal consolidation. The braid diameter and yarn angle were characterized before and after pultrusion. Results suggested that internal consolidation contributes to the preservation of the braid architecture. The consolidation quality was assessed by microscopy and per ASTM D3171 and showed void content lower than 4%.

1 INTRODUCTION

Composite hollow structures are widely used in many industrial applications such as aerospace, automotive, and sports. These structures offer the primary advantage of being lightweight while demonstrating high mechanical performance [1]. Hollow composite structures are typically manufactured by using the prepreg bladder moulding process [2]. This manufacturing process involves manually wrapping of prepreg materials around an inflatable bladder. Subsequently, the assembly is placed inside a mold defining the hollow structure's external surface. The internal pressure is achieved by pressurizing the bladder, causing the prepregs to be pressed outward for consolidation. After the curing process, the pressure on the bladder is released and it collapses [3]. This manual process requires highly skilled operators. Therefore, the mass production of hollow structures needs an automated process to reduce manufacturing costs.

Pultrusion is an automated manufacturing process that allows mass production of structures with constant cross-sections and high fibre volume fractions [4]. Pultruded products have exceptional mechanical, chemical, and structural properties and are employed in a variety of industries [5]. Pultrusion of continuous fibre reinforced composites with thermoset polymer matrices is a well-established manufacturing process. The use of thermoplastic polymers has greater benefits because of their superior toughness and damage tolerance, recyclable nature, and ability to be linked via welding [4]. However, the high viscosity of melted thermoplastics compared to thermosets makes processing these polymers more difficult. To try to compensate for the high viscosity of thermoplastic, several hybrid yarn technologies have been developed [5]. They effectively reduce the flow distance needed to impregnate the reinforcement fibres since the polymer is integrated with the reinforcement in the same yarn. DREF yarns are one of the composite hybrid yarns that consist of a continuous fibre core onto which discontinuous polymer fibres are spun using the friction spinning process [6]. The advantages of DREF yarns are good polymer/fibre distribution and better handling compared to other types of hybrid yarns.

In a standard non-reactive thermoplastic pultrusion, bobbins of hybrid yarns are placed in a creel that controls the unwinding tension [7]. These yarns are then pulled through a preheater, a heated die, then a cooling system, by the means of a puller. A saw is placed at the end of the manufacturing line to cut the finished products. The heated die is where melting and impregnation happen. The conventional thermoplastic pultrusion die consists of a tapered region designed to generate impregnation pressure [8]. The die then transitions to a constant region that shapes the product. Lastly. the pultrudate enters a cooling die where the composite is kept under pressure while the temperature cools down. The objective is to prevent deconsolidation and favour shrinkage to release the pultruded profile from the die surface [9]. Recently, multiple heated dies placed in sequence with a descending final cross-section were used to improve impregnation of thermoplastic composites. This process is called multi-die pultrusion [7], [9]–[13].

Braid-trusion combines a braiding machine with a pultrusion line to continuously produce structures with constant cross-section and off-axis fibre orientation [13]. Braiding is a textile technique that have received great attention in composites manufacturing due to the braid's mechanical properties, such as good fatigue and crush resistance properties [14]. Triaxial tubular braids, feature axial yarns that serve the purpose of enhancing dimensional stability and improving the longitudinal mechanical properties of the fabric [13]. Previous studies have shown that braided fibre orientation changes between the braided preform and the pultruded composite [13]. Another occurring event in braid-trusion is fibre waviness. It is characterised by local misalignment of fibres, consisting in a deviation of the nominal or intended fibre direction. Fibre waviness can have a detrimental effect on the mechanical properties of the composite [15]. When using thermoplastic composite hybrid yarns, the polymer filaments contained in the hybrid yarns melt in the hot dies, leaving more space for the reinforcement fibres to move. At the same time, the exterior fibres of the braid will experience intense friction on die walls that can lead to fibre waviness. While braid-trusion of full beams is a complex process, braid-trusion of hollow structures using concurrent internal and external tooling is a bigger challenge. Consolidation of the thermoplastic composite braid can be made using tapered dies compressing the braid onto a straight mandrel as evidenced in the existing literature [16]–[19]. That approach is referred as the external consolidation. To the best of the authors' knowledge, no studies were found using the alternate approach that could be called the internal consolidation. For internal consolidation, the mandrel is expanding into constant cross-section dies. Therefore, the objective of this study is to demonstrate the pultrusion of hollow braided structures using the internal consolidation approach. Braid-trusion experiments were done with the classic external consolidation and compared to the internal consolidation approach. The impact on the braid's morphology after manufacturing was measured.

2 METHODS

2.1 Materials

The DREF tows were made by friction spinning at Filspec Inc., Canada. These DREF tows were composed of a S2-Glass (GF, 933, AGY, density = 2.46 g/cm3) core of 66 tex. The glass core was surrounded by 25 tex of discontinuous PolyEthylene Terephthalate filaments (PET, staple fibre, Huvis Corporation). The tows' nominal glass fibre volume ratio was 50%. PET thermal properties were characterized in another study [20]. The glass transition temperature T_g, the melting temperature T_m and the degradation temperature T_d were 80°C, 256°C and 290°C respectively. The total yarn filaments cross-section area A_{yarn} was calculated using the fineness F (tex or g/km) divided by the density ρ for each of the reinforcement and matrix constituents of the yarn. The tow's reinforcement area A_{fibre} was 0.02683 $mm^2$and the tow's matrix area A_{matrix} was 0.02749 mm^2.

2.2 Pultrusion apparatus and process

Figure 1a. illustrates the schematic of the pultrusion apparatus. The first component was the pultrusion mandrel cantilevered from a fixed plate, followed by a rectangular shaped preheating chamber wrapped with a controlled heating tape set at 180°C. Rollers were placed upstream of the preheating chamber to keep the mandrel centred into the die cavities. Multiple heated dies were used to heat and shape the structure at 280°C. Fans were installed to cool down the thin-walled tube of the last die. Cartridge heaters were embedded in pultrusion dies and were controlled using the feedback from type J thermocouples placed close to the die moulding surfaces. The braid was pulled through a puller system along the line at 50 mm/min. The desired pultruded structures were a hollow rectangle, which lead to the use of rounded rectangular mandrels and die cavities. The total mandrel length was 1.22 m.

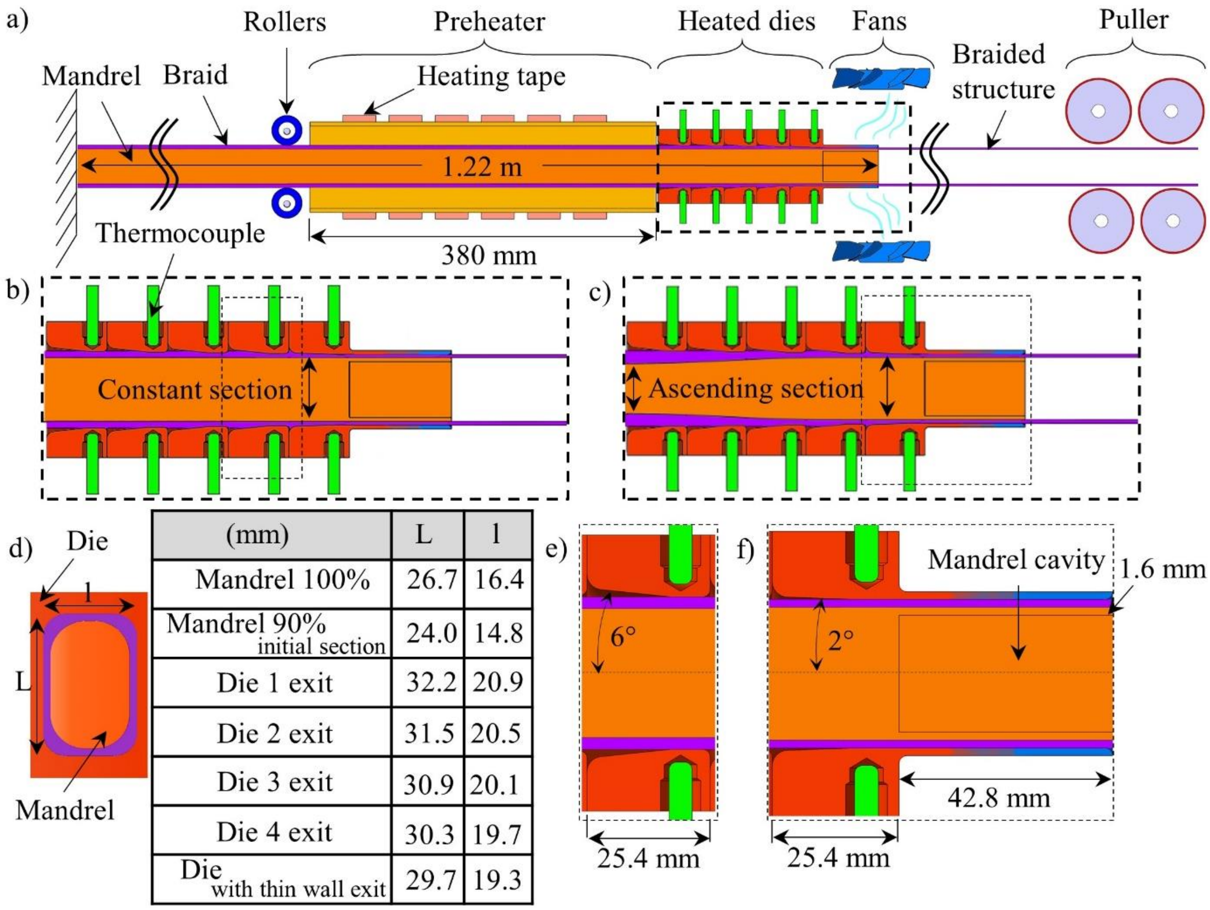

(mm)	L	l
Mandrel 100%	26.7	16.4
Mandrel 90% initial section	24.0	14.8
Die 1 exit	32.2	20.9
Die 2 exit	31.5	20.5
Die 3 exit	30.9	20.1
Die 4 exit	30.3	19.7
Die with thin wall exit	29.7	19.3

Figure 1: Comprehensive schematic view of the pultrusion apparatus. Figure 1a. The schematic of the pultrusion apparatus. Figure 1b. The set up for the external consolidation. Figure 1c. The set up for the internal consolidation. Figure1d. A transverse cross-section of a die and mandrel, with a table showing their dimensions. Figure 1e. A closer cross-section view of a heated die. Figure 1f. A closer cross-section view of the last die.

Two types of consolidation techniques were used and thus two sets of mandrels were used. Figure 1b and Figure 1c illustrates a closer view of a cross-section of the dies along the pultrusion line axis. Figure 1b illustrates the mandrel and dies set up for the external consolidation only. The mandrel has a constant cross-section all along. Figure 1c shows the mandrel and dies set up for the internal consolidation. In this set up the mandrel has an ascending cross-section with an initial circumference of 90% its finale one. For both set ups the same dies arrangement was used. Figure 1d illustrates a transverse cross-section of a die and mandrel, with a table showing their dimensions. The dies exit cross-sections decrease gradually with an area decrease ratio of 4%. Figure 1e. illustrates a closer cross-section view of a heated die. Each heated die had a 6° tapered section of 17.4 mm and a straight section of 8 mm. Figure 1f. illustrates a closer cross-section view of the last die with the thin-walled tube. This die had a thin-walled rectangular tube of 1.6mm thick and 42.8 mm long protruded from its cavity. The cooling die had a 2° taper angle. The mandrel was made hollow from the cooling end to limit heat conduction from the heated section to the cooling section. This thin-walled cooling method was detailed in reference [9].

2.3 Braid-trusion design

Table 1 presents the braid parameters for both braids along with the Braided Structures fibre volume fraction with the overfilling ratio at the last die exit. Three braid layers were manufactured for each braid. Each layer was a regular pattern braid (2/2) composed of 24 braiding yarns and 12 axial yarns. To achieve the desired pultruded shape, four larger axial yarns were placed at the corners. That means in the width direction (l), two big axial yarns were separated by one small axial yarn. In the length direction (L) two big axial yarns were separated by three small axial yarns. The braiding machine rotational and pulling speeds were set to obtain a braid pitch of 80 mm. The pitch is the distance travelled by one braiding yarn to complete one full rotation around the braid axis. Table 1 presents the average measured pitch (p) for each layer. The diameter of the braid (D) was constrained by a circular mandrel used for braiding. mandrel. Braid 100% was braided on a mandrel with a 25.4 mm diameter and was pultruded with the constant section mandrel. Braid 90% was braided on a mandrel with a 22.23 mm diameter and was pultruded with the ascending section mandrel. Table 1 presents the measured average circumference (C) for each layer, measured on the braid surface. The braid angle α shown in the Table 1 is the calculated average braid angle, by the relation,

$$\tan\alpha = {}^{\pi D}/_{p} = {}^{C}/_{p} \tag{1}$$

The crimp ratio (R_c) refers to the ratio of the actual interlaced length of a braiding yarn (L) over the spiral length (l) of the braiding yarn when projected on the circumference [21]. The crimp ratio for each layer is presented in Table 1 and calculated by the equation,

$$R_c = {}^{L}/_{l} \times 100\% = {}^{L \times p}/_{\cos\alpha} \times 100\% \tag{2}$$

An important parameter in pultrusion is the die filling ratio. This ratio should exceed 100% to insure consolidation during pultrusion. Table 1 presents the total calculated filling ratio R_f and is expressed by the equation,

$$R_f = {}^{A_{material}}/_{A_{exit}} \times 100\% \tag{3}$$

where $A_{material}$ is the materials yarns cross-section area at die entrance. A_{exit} the available exit area between the die and the mandrel. The material cross-section area is influenced by the angle α and the crimp ratio R_c of the braid according to,

$$A_{material} = \frac{24N_S\, A_{yarn}\, R_c}{\cos\alpha} + 8N_S\, A_{yarn} + 4N_B\, A_{yarn} \tag{4}$$

where A_{yarn} is the total yarn cross-section area calculated using the material cross-section area A_{fibre} and A_{matrix} [13]. N_S is the number of DREF tows in the braiding yarns and small axial yarns for each layer. N_B is the number of DREF tows in the large axial yarns for each layer.
Table 1 presents the calculated theoretical fibre volume content for the composite, and it was calculated according to,

$$V_f = {}^{A_f}/_{A_{exit}} \times 100\% \tag{5}$$

where A_f is the total fibre area is calculated using equation (4) with only the reinforcement area instead of the total yarn area.

	Braid 100%			Braid 90%		
Layer	1	2	3	1	2	3
N_S	16	16	24	16	16	24
N_B	64	64	64	64	64	64
Braid pitch p (mm)	83.8±2.0	81.5±1.5	82.8 ±0.8	83.1±0.9	80.5±0.9	78.9 ±1.0
Braid outside circumference C (mm)	94.5±0.9	109.7±1.5	127.2 ±0.4	88.4 ±0.15	100.5±1.1	120.5 ±0.2
Braid angle α °	46.2±0.7	51.4±0.5	55.0±0.3	43.5±0.2	49.5±0.3	54.4±0.3
R_c	103%	102%	103%	106%	102%	105%
R_f		104%			103%	
V_f		57%			56%	

Table 1: Braids preform parameters for both braided structures.

2.4 Characterization

Samples were cut from each pultruded structure for the analysis and evaluation of both internal and external surfaces after pultrusion. Each rectangular sample was cut along its length and width using a precision saw. The surfaces were manually polished using a 600-grit sandpaper to enhance the yarns visibility. Surfaces were observed under optical microscope (VHX700, Keyence) using 20x magnification.

The fibre pitch was measured on all four sides of the polished surfaces, by measuring the axial distance of 12 braiding yarns with the same spiral orientation. Circumference measurements were taken on four locations of the pultruded structures for each braid. Cross-sectional surfaces were observed under optical microscope using 20x magnification. Using microscopes measuring tools, external and internal circumferences were measured.

Samples were cut at their cross-sections for each pultruded structure for impregnation state analysis. Samples were then dried, imbedded in epoxy, and polished. Polished surfaces were observed and analysed under optical microscope using 200x magnification.

The pultruded structures constituent volume fractions (V_f, V_m and V_v) were measured by ignition, according to the procedure G of ASTM D3171-99. Where V_f is the fibre volume fraction, V_m is the matrix or polymer volume fraction, and V_v is the void content. The actual density of the pultruded structures was measured using method B of ASTM D792.

3 RESULTS

Hollow thermoplastic braided structures were pultruded using multi-die braid-trusion. The pultrusion experiments of Braid100% and Braid90% were not interrupted. No macro deformation of the braid at the pultrusion die entrance was observed. This observation indicates that the pultrusion process could have been performed continuously. The absence of blockage caused by the accumulation of the deformed braid at the die entrance supports this observation.

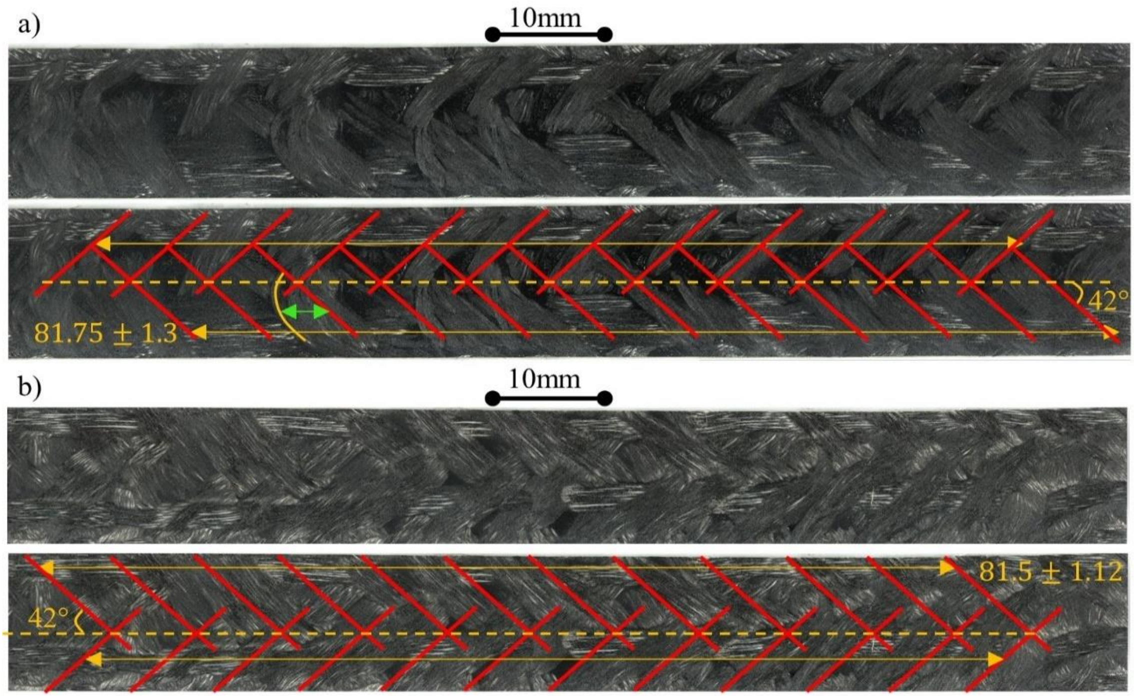

Figure 2: Internal surface of the Braided Structures after pultrusion Figure 2a Internal surface of the Braided Structure 100%. Figure 2b Internal surface of braided structure 90%.

Both consolidation approaches succeeded in the manufacturing of hollow thermoplastic composite structures. Fibre waviness on the external surfaces was present in both cases. Figure 2 presents the internal surface of the Braid100% (Figure 2a) and Braid90% (Figure 2b) after pultrusion. For each braid, the top figure is an unedited image of the internal surface. The bottom figure is an image of the internal surface with the calculated angle and pitch, highlighting the variation and waviness of the fibres. As shown in Figure 2a of the internal Braided Structure 100%, fibre waviness is present. On the internal Braided Structure 90% in Figure 2b, it appears that fibre waviness was less present. This observation tends to confirm that expanding the mandrel during braid-trusion has a positive impact on the waviness reduction. As the polymer component of the DREF yarn melted, the glass fibre tows became loose in the melted polymer pool. The mandrel expansion effectively applied tension to the braiding yarn, resulting in reduced waviness of the glass fibre tows.

3.1 Braid geometry measurements

Table 2 presents the average measurements for both braided structures after pultrusion for the internal and external layer. For both structures, average measured values of the pitch and circumferences were presented. The standard deviation was provided for the taken measurements. Internal and external angles were calculated using equation (1). Errors were calculated using proper error propagation equations.

	Braided Structure 100%	Braided Structure 90%
Internal braid pitch $p_1(mm)$	81.8 ± 1.3	81.5 ± 1.1
Internal circumference $C_1(mm)$	72.6 ± 0.3	72.8 ± 0.2
Internal braid angle α_1°	41.6 ± 0.3	41.8 ± 0.7
External braid pitch $p_2(mm)$	82.7 ± 0.5	81.7 ± 2.6
External circumference $C_2(mm)$	88.0 ± 0.8	87.9 ± 0.4
External braid angle α_2°	46.8 ± 1.3	47.1 ± 1.6

Table 2: Measurement on the Braided Structures after pultrusion

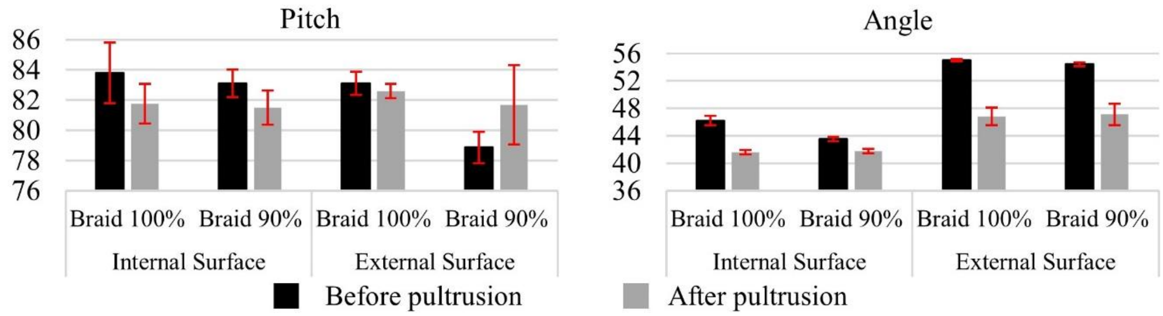

Figure 3: Bar graphs shows braids and braided structures parameters. Figure 3a Bar graph shows the measured pitch of braids before and after pultrusion. Figure 3b Bar graph shows the calculated angle of braids before and after pultrusion.

Figure 3 presents bar graphs comparing the pitch and angle of the braids before and after pultrusion. Figure 3a displays diverse average measures of pitch values with wide standard deviations for the internal and external surfaces of braid 100% and 90%. For the internal braided structure pitch p_1, decreased form 83.8 mm 81.8 mm for the Braided Structure 100%, and from 83.1 mm to 81.5 mm for the Braided Structure 90%. On the external braided structure, the pitch p_2 changed from 82.8 mm to 82.7 mm for the Braided Structure 100% and increased from 78.9 mm to 81.7 mm for the Braided Structure 90%. Since the averages varied withing the bounds of the standard deviations, it can be deduced that the observed pitch changes are not significant. The non-significant pitch change aligns with the observation that there was no accumulation of the deformed braid at the die entrance.

Figure 3b displays calculated angle values with narrow standard deviations for the internal and external surfaces of braid 100% and 90%. For the internal braided structure angle α_1, the values decreased from 46.2° to 41.6° for the Braided Structure 100%, although for the Braided Structure 90%, the angle slightly decreased from 43.5° to 41.8°, indicating that the change was not significant in comparison. These results suggest that due to the mandrel expansion, the braid preserved its architecture. For the external braided structure angle α_2, the values decreased from 55.0° to 46.8°. Similar to the external angle for the Braided Structure 90%, that decreased from 54.4° to 47.1°. The angle decrease is apparent solely due to the application of equation (1). Regardless of the fibre orientation, a decrease in the circumference leads to a reduction in the area occupied by the fibres, thereby inducing a significant increase in fibre waviness, which corresponds with the observed results.

3.2 Cross-sectional observation

Figure 4 shows typical micrographs at 200 magnifications for the Braided Structures 100% and 90% after pultrusion. Dark or black areas correspond to the voids. Light grey areas correspond to the PET polymer. The small round parts correspond to the glass fibres. Figure 4a shows multiple glass tows with black area at their centre indicating that these tows were not impregnated with the PET. Figure 4b show less unimpregnated glass tows. These results seem to indicate that the internal consolidation process enhances impregnations level.

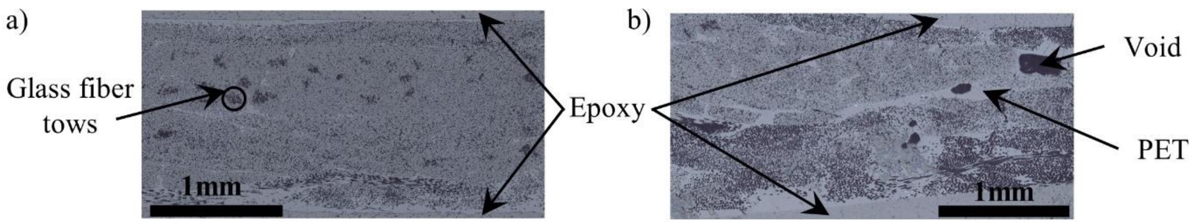

Figure 4: Typical micrographs of the polished cross section surface obtained from the pultruded braided structure. Figure 4a. Braided structure 100%. Figure 4b. Braided structure 90%

3.3 Constituent content

Predicted fibre volume content was 57% and 56% for the braid 100% and 90% consecutively, as presented in Table 1. Table 3 shows that the actual fibre volume fraction was noticeably higher than the initial prediction with 62% and 64% for the braid 100% and 90% respectively. In addition, there was an absence of fibre breakage during the pultrusion process. However, this apparent increase in fibre volume fraction suggests that the predicted V_f was inaccurate. The predicted V_f did not consider changes in angles and fibre waviness after pultrusion resulting in a wrongful prediction. This indicates that a more accurate hollow triaxle braid-trusion design should be developed to obtain more precise predicted values for the desired braided structure. Void content was lower than 4% for both braided structures. These results indicate that both structures were well impregnated.

	Braid 100%	Braid 90%
V_f	$62 \pm 0.32\%$	$64 \pm 1.52\%$
V_m	$35 \pm 0.189\%$	$34 \pm 1.67\%$
V_v	$3 \pm 0.14\%$	$2 \pm 0.15\%$

Table 3: The constituent content for each of the Braided Structures

4 CONCLUSION

The braid-trusion of hollow rectangular structures using two consolidation methods, internal and external consolidation, have been investigated. Triaxial braids were braided on different mandrel sizes. Braids were then pultruded using a multi-die process and a cantilevered mandrel. For external consolidation, the mandrel had a constant cross-section all along. For internal consolidation, the mandrel had an ascending cross-section with an initial circumference of 90% its finale one. During braid-trusion, it is notable that there were no interruptions of the process, which is due to the limited braid architecture changes. Characterisation of braid pitch, circumference and angle were made both before and after the pultrusion. For the internal consolidation, with the increase of the internal circumference the braided glass fibres were tensioned therefore reducing their waviness compared to the external consolidation experiment. Internal consolidation demonstrates that it is an effective approach for hollow braid consolidation. In future studies, a comprehensive braid design methodology will be developed for braid-trusion using the internal consolidation approach.

ACKNOWLEDGEMENTS

This work was supported by The Natural Sciences and Engineering Research Council of Canada [NSERC, RDCPJ 543847-19]; PRIMA Quebec [R18-13-003]; FilSpec Inc; Pultrusion Techniques; and Bauer Hockey ltd.

.

REFERENCES

[1] M. Naeimirad, R. Abuzade, V. Babaahmadi, R. E. Neisiany, R. Brüll, et F. Pursche, « Hollow fibre reinforced polymer composites », dans *Fibre Reinforced Composites*, K. Joseph, K. Oksman, G. George, R. Wilson, et S. Appukuttan, Éd. Woodhead Publishing, 2021, p. 461-477.

[2] S. K. Bhudolia, G. Gohel, J. Kantipudi, K. F. Leong, et P. Gerard, « Mechanical performance and damage mechanisms of thin rectangular carbon/ Elium® tubular thermoplastic composites under flexure and low-velocity impact », *Thin-Walled Struct.*, vol. 165, nº April, p. 107971, 2021, doi: 10.1016/j.tws.2021.107971.

[3] A. Brent Strong, Éd., *Fundamentals of Composites Manufacturing, Materials, Methods, and applications*. Dearborn, Michigan, 2008.

[4] P. K. Mallick, *Fibre-reinforced composites materials, manufacturing and design*, vol. 20, nº 2. 2007.

[5] K. Minchenkov, A. Vedernikov, A. Safonov, et I. Akhatov, « Thermoplastic pultrusion: A review », *Polymers*, vol. 13, nº 2. 2021, doi: 10.3390/polym13020180.

[6] M. Kurban, O. Babaarslan, et I. H. Cagatay, « Hybrid Yarn Composites for Construction », dans *Textiles for Advanced Application*, London, United Kingdom: Bipin Kumar, Suman Thakur, 2017.

[7] F. Lapointe et L. Laberge Lebel, « Fibre damage and impregnation during multi-die vacuum assisted pultrusion of carbon/PEEK hybrid yarns », *Polym. Compos.*, vol. 40, nº S2, p. E1015-E1028, 2019, doi: 10.1002/pc.24788.

[8] W. Michaeli et D. Jürss, « Thermoplastic pull-braiding: Pultrusion of profiles with braided fibre lay-up and thermoplastic matrix system (PP) », *Compos. Part A Appl. Sci. Manuf.*, vol. 27, nº 1, p. 3-7, 1996, doi: 10.1016/1359-835X(95)00004-L.

[9] N. Alsinani, M. Ghaedsharaf, et L. Laberge Lebel, « Effect of cooling temperature on deconsolidation and pulling forces in a thermoplastic pultrusion process », *Compos. Part B Eng.*, vol. 219, nº April, p. 108889, 2021, doi: 10.1016/j.compositesb.2021.108889.

[10] F. Lapointe, A. Oswald, et L. Laberge Lebel, « Manufacturing of carbon/polyamide beam by vacuum assisted pultrusion », dans *ECCM17-17th European confrence on composite materials*, 2016, p. 1-9.

[11] A. Oswald, F. L. Lapointe, et L. Laberge Lebel, « Multi-die, vacuum assisted pultrusion of flax/PLA thermoplastic biocomposite rods. », 2016.

[12] M. Ghaedsharaf, J. E. Brunel, et L. Laberge Lebel, « Thermoplastic composite rod manufacturing using biaxial braid-trusion », *ECCM 2018 - 18th Eur. Conf. Compos. Mater.*, 2018.

[13] L. L. Lebel et A. Nakai, « Design and manufacturing of an L-shaped thermoplastic composite beam by braid-trusion », *Compos. Part A Appl. Sci. Manuf.*, vol. 43, nº 10, p. 1717-1729, 2012, doi: 10.1016/j.compositesa.2012.03.001.

[14] M. Okano, A. Nakai, et H. Hamada, « Axial crushing performance of braided composite tubes », *Int. J. Crashworthiness*, vol. 10, nº 3, p. 287-294, 2005, doi: 10.1533/ijcr.2005.0347.

[15] M. P. Alves, C. A. Cimini Junior, et S. K. Ha, « Fibre waviness and its effect on the mechanical performance of fibre reinforced polymer composites: An enhanced review », *Compos. Part A Appl. Sci. Manuf.*, vol. 149, nº November 2020, 2021, doi: 10.1016/j.compositesa.2021.106526.

[16] A. Memon et A. Nakai, « Mechanical properties of jute spun Yarn/PLA tubular braided composite by pultrusion molding », *Energy Procedia*, vol. 34, p. 818-829, 2013, doi: 10.1016/j.egypro.2013.06.818.

[17] P. Wongsriraksa et A. Nakai, « The Effect of Process Parameters on Impregnation Properties of

Pultruded Carbon Fibre Reinforced Thermoplastic Epoxy Composites », *ECS Trans.*, vol. 88, nº 1, p. 177-185, 2018, doi: 10.1149/08801.0177ecst.

[18] T. Saito, A. Nakai, et A. Ohtani, « Effects of fabrication method of composite yarn intermediate material and resin melt viscosity on the impregnation properties and mechanical properties of PA66 fibre and glass fibre composites », *J. Thermoplast. Compos. Mater.*, 2020, doi: 10.1177/0892705720964559.

[19] J. Schäfer, T. Gries, R. Schuster, et C. Lammel, « Continious production of fibre reinforced thermoplastic composites by braiding pultrusion », *ICCM Int. Conf. Compos. Mater.*, vol. 2015-July, nº July, p. 19-24, 2015.

[20] N. Cordona, « Consolidation of DREF precursor yarns for manufacturing glass fibre-polyethylene terephthalate thermoplastic composites », Polytechnique Montreal, 2023.

[21] D. Yang, « Investigation of Braid Geometry for Complex Braided Composite Structures », University of Manchester, 2018.